Chemistry Research Journal, 2017, 2(1):46-56

Available online www.chemrj.org

Research Article

ISSN: 2455-8990
CODEN(USA): CRJHA5

GC-MS and Molecular Docking Studies for Identification of Anti-malarial Compounds in Agbo-Iba PMII-a Polyherbal Formulation

Pass Iyamah[1], Ayodeji Famuti[2], MacDonald Idu[2]

[1]Department of Biology, College of Education, PMB1251 Warri, Delta State, Nigeria
[2]Department of Plant Biology and Biotechnology, University of Benin, Benin City, Edo State, Nigeria

Abstract Malaria prevalence is one of the life-threatening diseases responsible for more deaths around the world than any other parasitic disease. Due to the outbreak of strains that show resistance to the current synthetic anti-malarial arsenal, a large focus has been directed to structure based drug designing. The present study investigated the anti-malarial active constituents present in an ethanolic extracted polyherbal formulation (Agbo-iba PMII) comprising Sixteen (16) plants using GC-MS analysis and molecular docking studies of the identified compounds to determine the potential of the polyherbal formulation to treat malaria. The results revealed 42 phytochemical constituents derived from the GC-MS analysis. However, the result from the molecular docking studies done using Autodock/Vina show that 1,3-Diphenyl-2-azafluorene with a binding affinity of -10.2 Kcal/mol found only in *Azadirachta indica* holds more promising lead target formation against malaria. From the results obtained, it can be concluded that1,3-Diphenyl-2-azafluorene acts against malaria by blocking Methionyl-tRNA synthetase (MRS) and can further be developed into a potent drug for malaria.

Keywords Malaria, 1,3-Diphenyl-2-azafluorene, Gas Chromatography Mass spectrometry (GCMS)

1. Introduction

Malaria is one of the life threatening infectious diseases caused by protozoan parasite. Out of the five human *Plasmodium* species (*Plasmodium falciparum, P. vivax, P. ovale, P. knowlesi, and P. malariae)* (White, 2008), the major complication is caused by *Plasmodium falciparum* which appears to be more virulent. According to reports from the World Health Organization (WHO), about 438, 000 mortalities were recorded in the year 2015 as result of malaria of which 90 percent of the deaths occur in sub-Saharan Africa where Nigeria and the democratic Republic of Congo accounted for 35% of malaria Deaths [1]. Multidisciplinary scientific researchers are making the best efforts in fighting against the prevalence of this disease, but the sure best, perfect and efficient cure is yet to be discovered. The nulear genome form the machinery for the synthesis of protein of malaria parasite. These proteins are transported to its target to perform required functions [2]. The translation of the genetic code into polypeptide chains are primary facilitated by aminoacyl-tRNA synthetases (aaRSs). Aminoacyl-tRNA synthetases (aaRSs) ligate specific amino acid to its cognate tRNA which is then used in protein synthesis (Woese *et al.,* 2000). Aminoacyl-tRNA synthetases have gained a wide range of sequence, structural and functional diversity due to the course of evolution [3]**.** *Plasmodium falciparum* possess 36 aaRSs that show an asymmetric distribution among parasite organelles [4-7]. The presence of appended domains imparts characteristic functions to parasitic aaRSs [6-8]. Malaria parasite aaRSs are recently been explored as new targets for drug development [9-11]. Within aaRSs, Methionyl-tRNA synthetase (MRS) can serve as valuable drug targets because of their sequence and domain

heterogeneity [11]. Malaria parasite Methionyl-tRNA synthetase (MRS) is being explored as new targets for drug development due to their sequenece and domain heterogencity [12]. Methionyl-tRNA synthetase (MRS) binds to free methionine in its catalytic site, where the amino acid is being charged due to the presence of ATP, which then is finally transferred to 2-OH moiety of the terminal adenosine of tRNA. MRS acylates (tRNAf Met and tRNAm Met) having nucleotide sequence with different nucleotide. Appearance of resistant strains of *P. falciparum* call for an urgent need to develop new anti-malarial drugs [9]. Management of Malaria with no side effects is still a challenge to the drug developers. Hence, Malaria prevalence continues to enkindle and sustain motivation in finding its cure. This leads to increasing demand for natural products from plant with antimalarial activity and fewer side effects as provided by the World Health Organization [13]. The present study is so designed to investigate the antimalarial active constituents present in an ethanolic extracted polyherbal formulation (Agbo-iba PMII) comprising Sixteen (16) plants using GC-MS analysis and molecular docking studies of the identified compounds to determine the potential of the polyherbal formulation to treat malaria.

2. Materials and Methods

2.1. Plant collection and Phytochemical Screening

2.1.1. Plant Material collection

Fresh parts of constituent plants of Agbo-iba including, the leaves of *Azadirachta indica, Cymbopogon, citratus, Mangifera indica. Carica papaya, Psidium guajava, Vernonia amygdalina, Ocimum gatissimum, Chromolaena odorata* and *Anacardium occidentale* and *Persea americana*; stem barks of *Enantia chlorantha* and *Alstonia boonei;* roots *of Morinda lucida* and *Nauclea latifolia,* and the fruit barks of *Citrus aurantifolia* and *Ananas comosus* were harvested from their natural habitats in Benin and Lagos, Nigeria.

2.1.2. Extraction of Plant Materials and preparation of the Poly-herbal remedy (Agbo-iba PMII)

One thousand (1000) g each of the sixteen (16) powdered plant material were exhaustively extracted using the soxhlet extractor in 100% ethanol, which was then concentrated in an air oven at 40 °C. The extracts were weighed and stored in labelled sealed plastic containers at 4 °C until use to prevent decomposition. Equal portion of each crude extracts were weighed and dissolved in DMSO4 followed by subsequent dilution to lower concentration of DMSO4 to <1% to avoid carry over (solvent) effect [14].

2.1.3. Gas Chromatography-Mass Spectrometry (GC-MS) Analysis

The gas chromatography–mass spectrometry (GC-MS) analysis of the polyherbal formulation was performed using a GC-MS (Modal; QP2010 series, Shimadzu, Tokyo, Japan) equipped with a VF–5ms fused silica capillary column of 30 m length, 0.25 mm diameter and 0.25 mm film thickness. For GCMS detection, an electron ionization system with ionization energy of 70 eV was used. Helium gas (99.99 %), a carrier gas at a constant flow rate of 1.51 N/min. Injection and mass transfer line temperature were set at 200 and 240 °C. The oven temperature was programmed from 70 to 22 °C at 10 °C/min, held isothermal for 1 min and finally raised to 300 °C at 10 °C/min. 2 ml of water solution of the samples was manually injected in the split less mode, with a split ratio of 1:40 and with mass scan of 50-600 amu. Total running time of GC-MS is 35 min. The relative percentage of each extract constituents were expressed as percentage with peak area normalization. Interpretation of mass spectrum of plant extracts were conducted using the data base of national institute of standard and technology (NIST) library having over 62,000 spectral patterns. The spectrum of the compounds was compared with the spectrum of the National Institute of Standard and Technology (NIST) library data base.

2.2. Modelling and *in silico* screening

2.2.1. Ligand (Compound) Preparation for Docking

2D structure of the ligand isolated from Sixteen (16) plants which makes up the polyherbal formulation (Agbo-iba PMII) was drawn using the ChemAxon software called Marvin Sketch (https://www.chemaxon.com/). To prepare the ligand for docking, it was then converted to 3-Dimensional structure with a force field of MMFF94.

2.2.2. Preparation of protein structure

To get the synthase domain of *Plasmodium falciparum* methionyl-tRNA synthetases, the sequences were matched with homologs of known structure using BLAST against PDB. This showed that methionyl-tRNA synthetases from *Thermos thermophilus* with a PDB ID of 3VU8, downloaded from database Protein Data Bank (*http://www.rcsb.org/pdb/explore/explore.do?structureId=3VU8)* have the nearest homolog and template for docking. The docking calculations was performed using Autodock/Vina [15-16].

2.2.3. Molecular Docking

Autodock vina 4.2 [16] was used to carry out the molecular docking. Auto Dock tool was used to calculate the ligand binding to methionyl-tRNA synthetases model using a grid spacing of 0.375 angstroms and the grid points in X, Y and Z axis were set at 60 × 60 × 60. The grid center coordinates was placed at X: 40.11, Y: 35.05, Z: 35.74. The grid box was placed at the binding site of the enzyme which gives enough space for the ligand rotation and translation **(Table 1&2)**. Results gotten from AutoDock were analyzed to study the binding energy and the interaction of the docked structure.

Table1: Grid center coordinate

Gridsetting	X	Y	Z
	40.11	35.05	35.74

Table2: Grid definition parameters

Parameters	Spacing	X-point	Y-point
	0.375	60	60

2.2.4. Docking confirmation using Mcule

Mcule speeds up early phase drug discovery by its integrated molecular modeling tools, computational capacity and high-quality compound database (https://mcule.com/dashboard/). Molecular docking using Mcule was done in the Structure-based virtual screen - Workflow builder. The ligand was uploaded in 2D. Protein which is the target was uploaded in 3D with a binding site center X: 40.11, Y: 35.05, Z: 35.74. The simulation was RUN with a maximum hit of 1000.

2.2.5. Experimental confirmation and (IC_{50}) Calculation

Experimental confirmation and IC50 Calculation was done using Chembl (https://www.ebi.ac.uk/chembl/). The target fasta file was copied from pdb (*http://www.rcsb.org/pdb/explore/explore.do?structureId=3VU8)* and uploaded at the Protein target BLAST search in Chembl. The target associated Bioactivities with Target Id of CHEMBL2870 having 127 compound was downloaded. To calculate the IC50, the target associated Bioactivities was dock against methionyl-tRNA synthetase with a config.txt parameter (Table 3). After docking the results was harvested by 'egrep'. The Coefficient was determined by plotting a graph shown in figure 5, of the docked score against the Pchembl value.

Table 3: The config.txt for Chembl moleculer docking using Auto/Vina

Center_x	Center_y	Center_z	Size_x	Size_y	Size_z	Number of modes
40.11	35.05	35.74	22.50	22.50	22.50	1

3. Results and Discussion

In the present study, Ethanolic extract of the polyherbal formulation (Agbo-iba PMII) was subjected to GC-MS analysis to identify the potential phytochemical constituents present (figure 1). In this study, the GC-MS analysis

show 42 compounds (table 4) found in the polyherbal formulation. The phytochemicals and the receptor 3VU8 were docked using Autodock/Vina which is used to predict the affinity, activity and the binding orientation of the phytochemicals. Analysis was done based on free energy of binding and lowest docked energy as shown in table 4. The phytochemical constituent found in each of the sixteen (16) plants which make up the 42 compounds found in the formulation were plotted against its dock value, as shown in Figure 2 . This is done to identify a lead compound out of the phytochemical constituents found in the polyherbal formulation having the highest binding affinity to the receptor.

According to the graph, 1,3-Diphenyl-2-azafluorene show the highest binding affinity of -10.2 Kcal/Mol as predicted by Autodock/Vina. The result was confirmed using Mcule (an online drug discovery platform). The mcule ID C-297566439 also gives a docking result of -10.1 Kcal/Mol, which therefore validate the Autodock/Vina docking result. From the result shown in figure 2, 1,3- Diphenyl-2-azafluorene was found only in *Azadirachta indica* Linn.

Docking analysis of 3VU8 with 1,3-Diphenyl-2-azafluorene enabled the identification of amino acid specific residues viz. MET1 GLU2 LYS3 VAL4 PHE5 TYR6 VAL7 THR8 THR9 PRO10 ILE11 TYR12 TYR13 VAL14 ASN15 ALA16 GLU17 PRO18 HIS19 LEU20 GLY21 HIS22 ALA23 TYR24 THR25 THR26 VAL27 VAL28 ALA29 ASP30 PHE31 LEU32 ALA33 ARG34 TRP35 HIS36 ARG37 LEU38 ASP39 GLY40 TYR41 ARG42 THR43 PHE44 PHE45 LEU46 THR47 GLY48 THR49 ASP50 GLU51 HIS52 GLY53 GLU54 THR55 VAL56 TYR57 ARG58 ALA59 ALA60 GLN61 ALA62 ALA63 GLY64 GLU65 ASP66 PRO67 LYS68 ALA69 PHE70 VAL71 ASP72 ARG73 VAL74 SER75 GLY76 ARG77 PHE78 LYS79 ARG80 ALA81 TRP82 ASP83 LEU84 LEU85 and GLY86 within and around the 3VU8 binding pocket to play an important role in the ligand binding affinity as shown in Figure 4 . The docking pose of 3VU8 and 1,3-Diphenyl-2-azafluorene is shown in Figure 3.

Our *in silico* experiments shows that 1,3-Diphenyl-2-azafluorene binds 3VU8, inhibits its function and thus may act as a potent anti-malaria drug. 1,3-Diphenyl-2-azafluorene has been reported to be found in *Azadirachta indica* Linn [17] but there has been no report on its use as a drug target against any protein. Making this study the first in the molecular docking of 1,3-Diphenyl-2-azafluorene against the *Plasmodium falciparum* MRS receptor

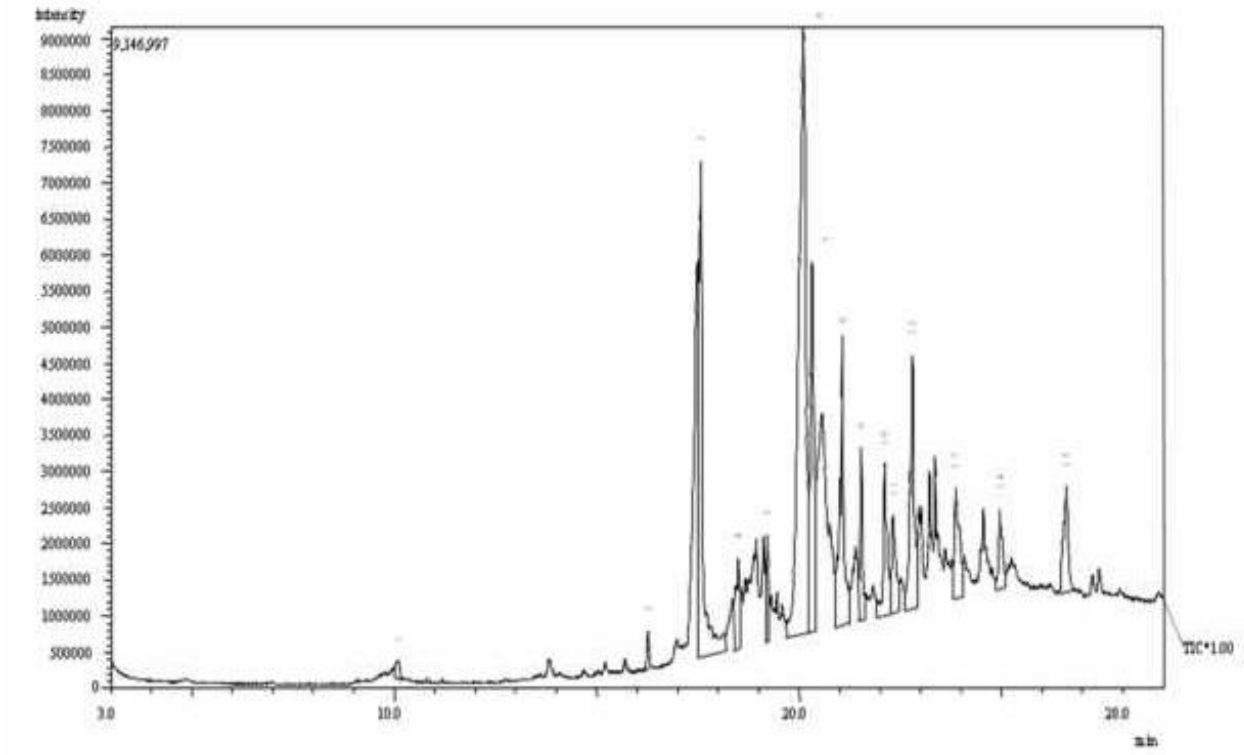

Figure 1: GC-MS analysis

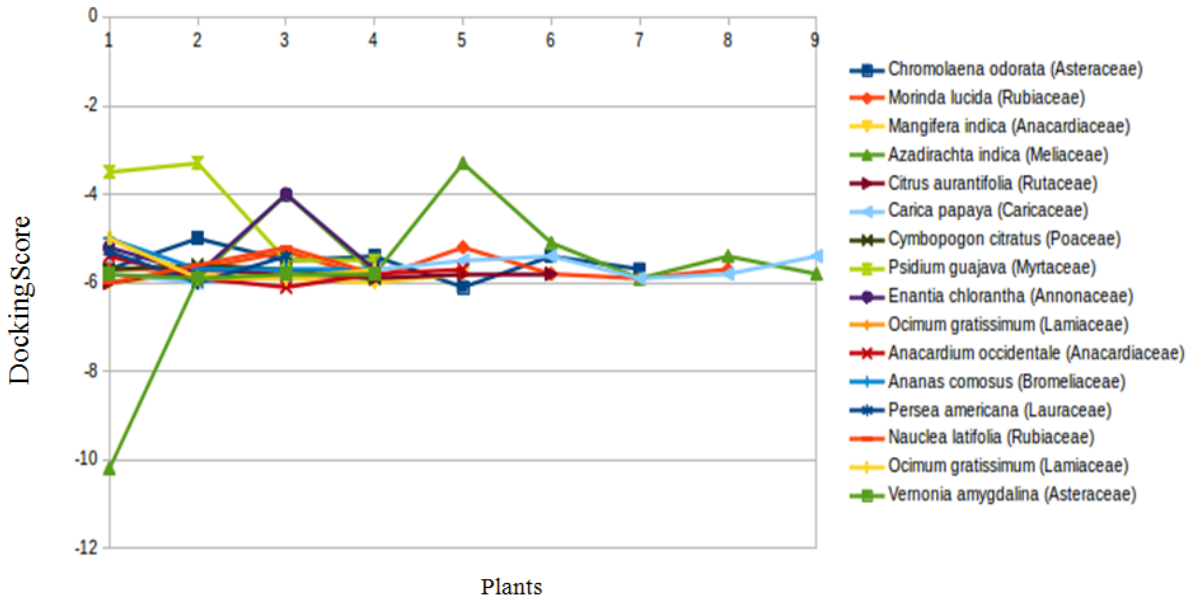

Figure2: Polyherbal formulation with the docked score

Table 4: Phytochemical constituent identified from GC-MS analysis of the polyherbal formulation

S/N	Name of compound	Molecular formula	Molecular weight g/mol	Structure
1.	2,3-Dihydroxypropyl	$C_{19}H_{38}O_4$	330	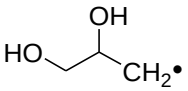
2.	2-butyl-1-octanol	$C_{12}H_{26}O$	186	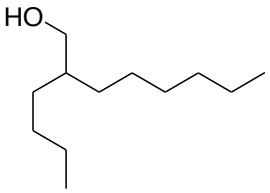
3.	2-dodecyl-1,3-propanediol	$C_{15}H_{32}O_2$	244	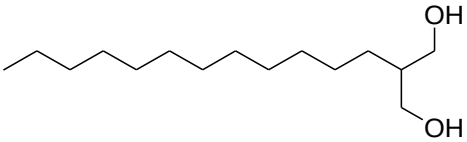
4.	1,3-Diphenyl-2-azafluorene	$C_{24}H_{17}N$	319.398	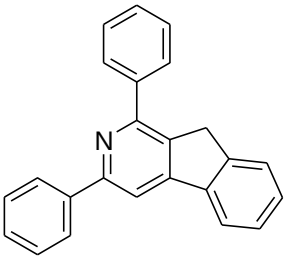
5.	3-Acetoxydodecane	$C_{14}H_{28}O_2$	228	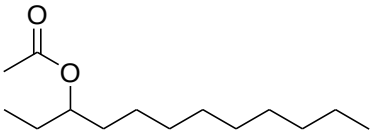

6.	4-Ethyl-5-methylnonane	$C_{12}H_{26}$	170	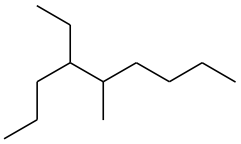
7.	4-Tridecene,(Z)	$C_{13}H_{26}$	182	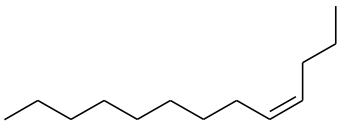
8.	6-octadecenoic acid	$C_{19}H_{36}O_2$	294	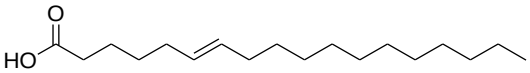
9.	9-octadecenal	$C_{18}H_{34}O$	266	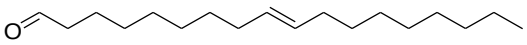
10.	9-octadecenoate	$C_{18}H_{34}O_2$	282	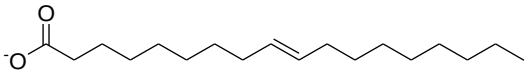
11.	11-Tridecen-1-ol	$C_{13}H_{26}O$	198	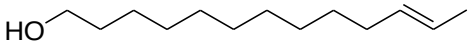
12.	11-Octadecenoic acid	$C_{19}H_{36}O_2$	296	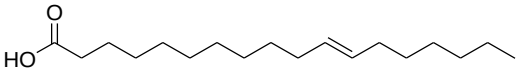
13.	Acetic acid	$C_{10}H_{20}O_2$	172	CH_3COOH
14.	Cis-9-Hexadecenal	$C_{16}H_{30}O$	238	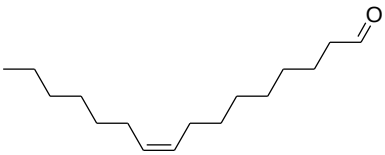
15.	Cis-13-Docosenoylchloride	$C_{18}H_{34}O$	266	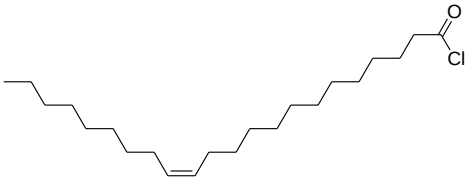
16.	Cis-13-octadecenal	$C_{18}H_{34}O$	266	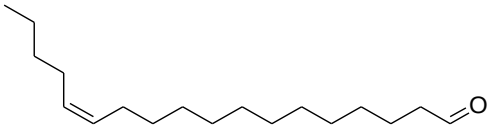
17.	1-fluorodecane	$C_{10}H_{21}F$	160	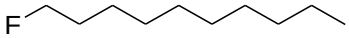
18.	9-octadecenoic acid	$C_{18}H_{34}O_2$	282	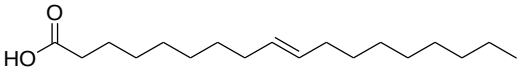
19.	Delta-13-cis-Docosenoic acid	$C_{22}H_{42}O_2$	338	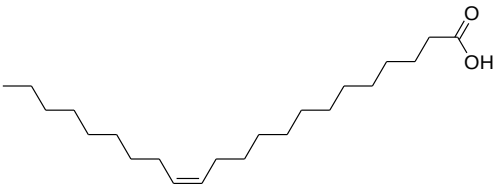
20.	Glycerol-1-monopalmitate	$C_{19}H_{38}O_4$	330.509	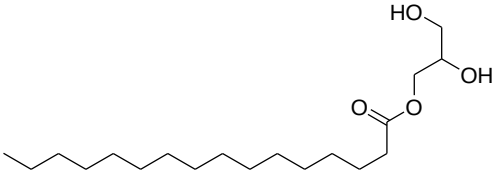
21.	Heptadecane	$C_{20}H_{42}$	282	

22.	Hexanoicacid 9-decen-l-yl ester	$C_{16}H_{30}O_2$	254	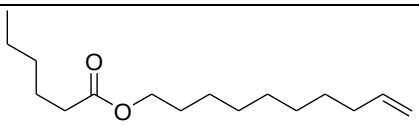
23.	n-hexadecanoic acid	$C_{16}H_{32}O_2$	256	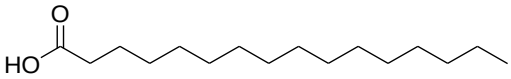
24.	Nonadecanoic acid	$C_{19}H_{38}O_2$	298	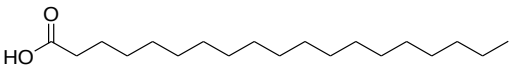
25.	Ethyl hexadecanoate	$C_{18}H_{36}O_2$	284	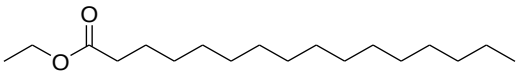
26.	Octadecanoic acid	$C_{22}H_{44}O_4$	372	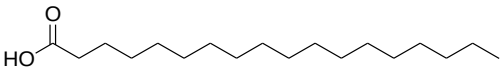
27.	Oxalic acid	$C_{20}H_{38}O_4$	342	$(COOH)_2$
28.	Palmitate	$C_{36}H_{60}O_2$	524.8	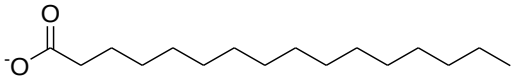
29.	Palmitic acid	$C_{17}H_{34}O_2$	270	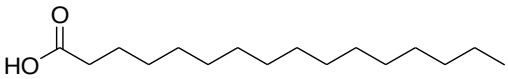
30.	Pentadecanecarboxylic acid	$C_{16}H_{32}O_2$	256	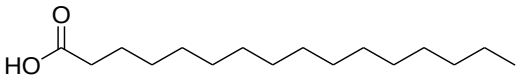
31.	Pentadecanoic acid	$C_{17}H_{34}O_2$	270.457	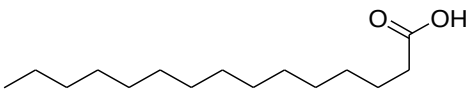
32.	Nonanoic acid	$C_{15}H_{30}O_2$	242	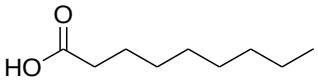
33.	Stearic acid	$C_{18}H_{36}O_2$	284	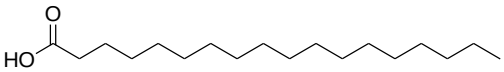
34.	Tridecanoic acid	$C_{14}H_{28}O_2$	228	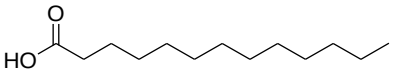
35.	Z-11-pentadecenal	$C_{15}H_{28}O$	224.38	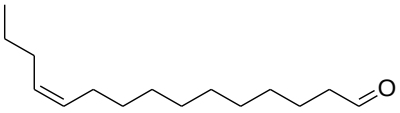
36.	1,2-Dipalmitoyl-sn-glycero-3-phosphoethanolamine	$C_{49}H_{86}N_5O_{15}P$	1016.2	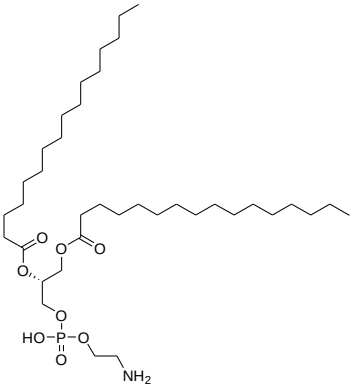

37.	Aquacera	$C_{22}H_{44}O_4$	372	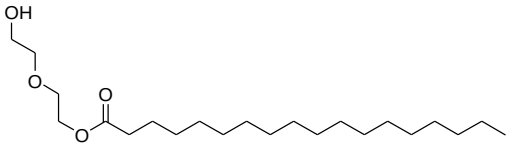
38.	Dipalmitoyl phosphoethanolamine	$C_{37}H_{74}NO_8P$	691.97	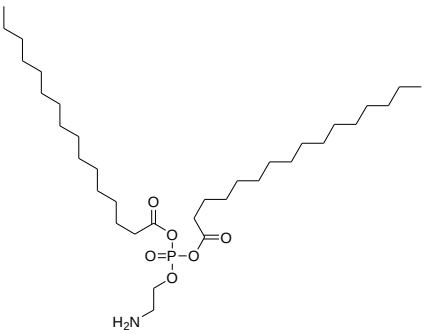
39.	Cis-9-Octadecen-1-ol	$C_{18}H_{36}O$	268.4	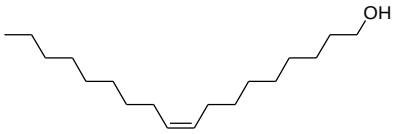
40.	Diisononyladipate	$C_{24}H_{46}O_4$	398.6	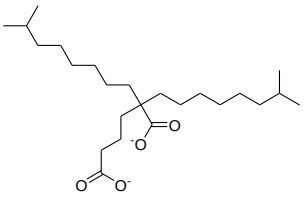
41.	Tetradecanoic acid	$C_{14}H_{28}O_2$	228.3	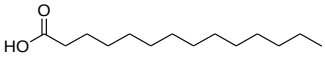
42.	Eicosanoic acid	$C_{20}H_{40}O_2$	312.5	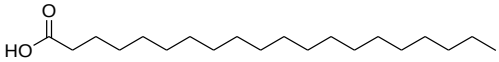

Table 5: Binding affinity of the phytochemical constituent of the polyherbal formulation

S/N	Compounds	Binding affinity (kcal/mol)
1.	1_2-Dipalmitoyl-sn-glycero-3 phosphoethanolamine.	-6.3
2.	1_3-Diphenyl-2-azafluorene.	-10.2
3.	2_3-Dihydroxypropyl.	-3.5
4.	2-butyl-1-octanol.	-5.2
5.	2-dodecyl-1_3-propanediol.	-5.7
6.	3-Acetoxydodecane.	-5.3
7.	4-Ethyl-5-methylnonane.	-5.0
8.	4-TrideceneZ_.	-5.0
9.	6-octadecenoic_acid.	-5.9
10.	9-octadecenal.	-5.4
11.	9-octadecenoate.	-5.9
12.	9-octadecenoic_acid.	-6.0
13.	11-Octadecenoic_acid.	-5.9
14.	11-Tridecen-1-ol.	-5.6
15.	13-Docosenoic_acid.	-5.6
16.	Aceticacid.	-3.3
17.	Aqua_Cera.	-5.9
18.	Cis-9-Hexadecenal.	-5.6
19.	Cis-9-Octadecen-1-ol.	-5.4

20.	Cis-13-Docosenoyl_chloride.	-5.7
21.	Cis-13-octadecenal.	-5.7
22.	Diisononyl adipate	-5.7
23.	Decane_1-fluoro.	-4.5
24.	delta_13-cis-Docosenoic_acid.	-5.9
25.	Dipalmitoyl_phosphoethanolamine.	-5.9
26.	Eicosanoicacid.	-5.7
27.	Ethyl_hexadecanoate.	-5.8
28.	n-hexadecanoic_acid.	-5.7
29.	Hexanoic acid 9-decen-l-ylester.	-5.2
30.	Nonadecanoic_acid.	-5.5
31.	Nonanoic_acid.	-5.1
32.	Octadecanoic_acid.	-5.2
33.	Oxalic_acid.	-4.0
34.	Palmitate.	-5.9
35.	Palmitic acid.	-5.7
36.	Pentadecanecarboxylic_acid.	-5.8
37.	Pentadecanoic_acid.	-5.8
38.	Stearic_acid.	-5.6
39.	Tetradecanoic_acid.	-5.7
40.	Tridecanoic_acid.	-5.4
41.	Z-11-pentadecenal.	-5.5
42.	Glycerol_1-monopalmitate.	-6.1

3D structure of
1,3-Diphenyl-2-azafluorene

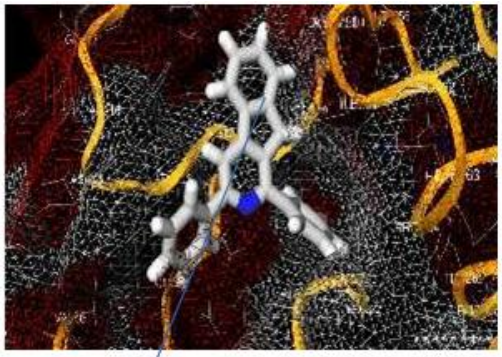

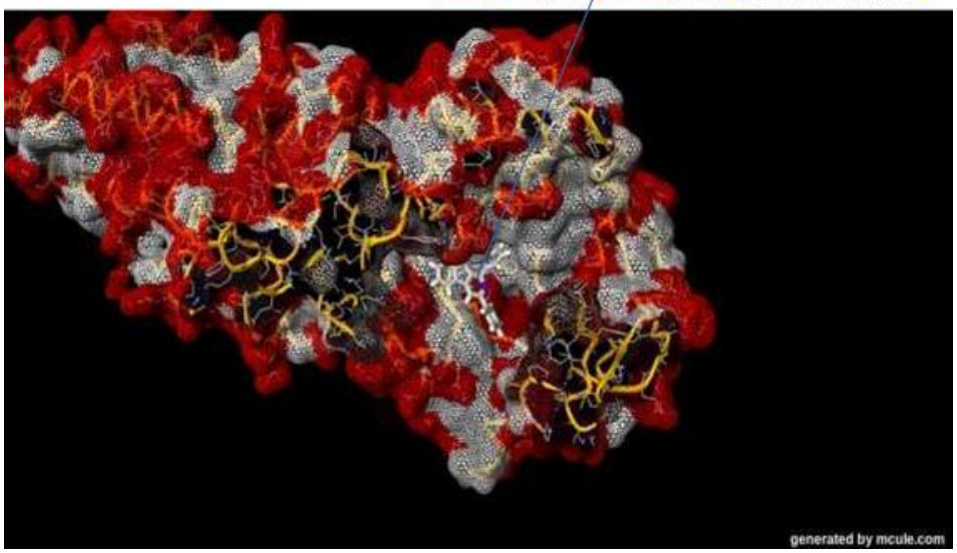

Figure 3: the moleculer binding poseof1,3-Diphenyl-2-azafluorenein methionyl-tR NA synthetases

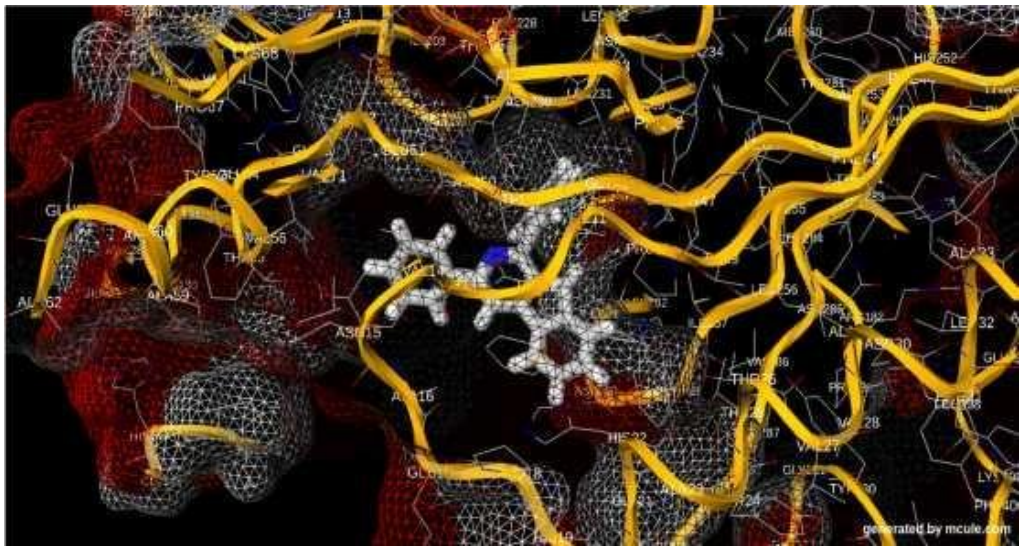

Figure 4: The amino acid residue of the binding pose of 1,3-Diphenyl-2-azafluorene in methionyl-tRNA synthetase

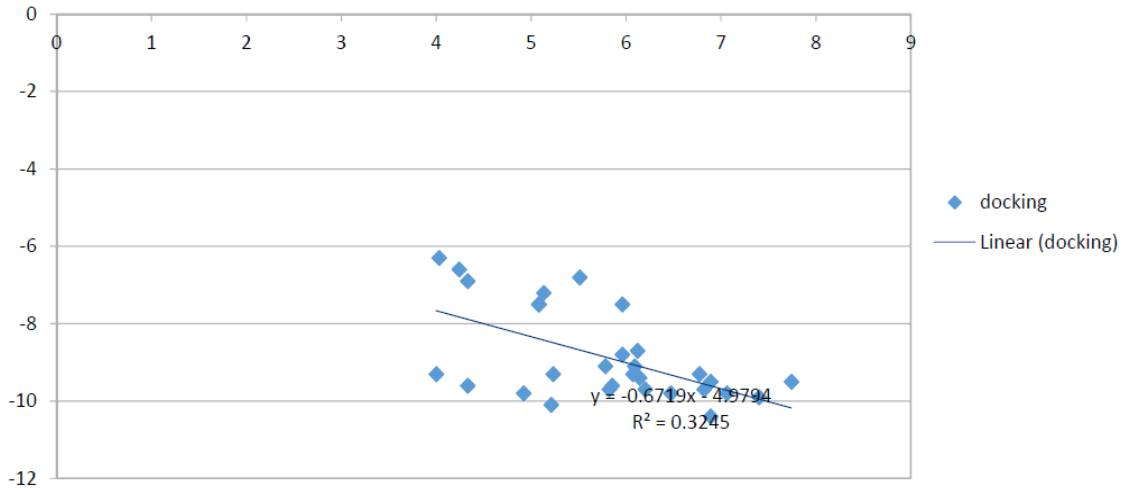

Figure 5: The coeffient of correlation of (IC_{50}) methionyl-tRNA synthetases

References

1. WHO: World Malaria Report 2015. Geneva: World Health Organization.
2. Johnson, R.A, McFadden, G.I, Goodman, C.D. (2011). Characterization of two malaria parasite organelle translation elongation factor G proteins: the likely targets of the anti-malarial fusidic acid. *PLoS One*, 6:e20633. 31.
3. *Mazauric, M.H., Keith, G., Logan, D., Kreutzer, R., Giegé, R., Kern, D. (1998). Glycyl-tRNA synthetase from Thermus thermophilus--wide structural divergence with other prokaryotic glycyl-tRNA synthetases and functional inter-relation with prokaryotic and eukaryotic* glycylation systems. *Eur. J. Biochem.* 251:744-757.
4. Khan, S., Sharma, A., Jamwal, A., Sharma, V., Pole, A.K., Thakur, K.K., Sharma, A. (2011). Uneven spread of cis- and trans-editing aminoacyl-tRNA synthe-tase domains within translational compartments *of P. falciparum*. *Sci Rep*1:188.
5. Jackson, K.E., Pham, J.S., Kwek, M., De Silva, N.S., Allen, S.M., Goodman, C.D., McFadden, G.I., De Pouplana, L.R., Ralph, S.A., (2012). Dual targeting of aminoacyl-tRNA synthetases to the apicoplast and cytosol in Plasmodium falciparum . *Int J Parasitol* 42: 177–186.

6. Jackson, K,E., Habib, S., Frugier, M., Hoen, R., Khan, S., Pham, J.S., Ribas de Pouplana, L., Royo, M., Santos, M.A., Sharma, A., Ralph, S.A. (2011). Protein translation in Plasmodium parasites. *Trends Parasitol* 27: 467–476.
7. Bhatt, T.K., Kapil, C., Khan, S., Jairajpuri, M.A., Sharma, V., Santoni, D., Silvestrini, F., Pizzi, E., Sharma, A. (2009). A genomic glimpse of aminoacyl-tRNA synthetases in malaria parasite Plasmodium falciparum. *BMC Genomics* 10: 644.
8. Bhatt, T.K., Khan, S., Dwivedi, V.P., Banday, M.M., Sharma, A., Chandele, A., Camacho, N., De Pouplana, L.R., Wu, Y., Craig, A.G., Mikkonen, A.T., Maier, A.G., Yogavel, M., Sharma, A. (2011). Malaria parasite tyrosyl-tRNA synthe- tase secretion triggers pro-inflammatory responses. *Nat Commun*, 2:530.
9. Khan, S., Garg, A., Camacho, N., Van Rooyen, J., Kumar, P. A, Belrhali, H., Ribas de Pouplana, L., Sharma, V, Sharma, A. (2013). Structural analysis of malaria-parasite lysyl-tRNA synthetase provides a platform for drug development. *Acta Crystallogr D Biol Crystallogr* 69:785–795.
10. Pham, J.S., Sakaguchi, R., Yeoh, L.M., De Silva, N.S., McFadden, G.I., Hou, Y.M., Ralph, S.A. (2014). A dual-targeted aminoacyl-tRNA synthetase in *Plasmodium falciparum* charges cytosolic and apicoplast tRNACys. *Biochem J* 458: 513–523.
11. Hussain, T., Yogavel, M. and Sharma, A. (2015). Inhibition of protein synthesis and malaria parasite development by Drug targeting of methionyl–tRNA synthesis. Antimicrob. Agents *Chemother*. 59:1856-1867.
12. Critchley, I.A., Green, L.S., Young, C.L., Bullard, J.M, Evans, R.J, Price, M., Jarvis, T.C., Guiles, J.W., Janjic, N., Ochsner, U.A. (2009). Spectrum of activity and mode of action of REP3123, a new antibiotic to treat Clostridium difficile infections. *J. Antimicrob. Chemother*. 63:954-963.
13. WHO: World Malaria Report 1985. World Health Organization.
14. Muthaura, C. N., Nkeriko, J. M., Mutai, C., Yenesew, A., Gathirwa, J. W., Irungu, B. N., Nyangacha, R., Mungai, G. M. and Derese, S. (2015). Anti-plasmodial potential of traditional phytotherapy of some renedies used in the treatment of malarial in Meru-Tharaka Nithi county of Kenya. *J Ethnopharmacol*, 175, 315-323
15. Trott, O. and Olson A. J., (2010) AutoDock Vina: improving the speed and accuracy of docking with a new scoring function, efficient optimization and multithreading, *Journal of Computational Chemistry* 31 455-461.
16. Morris, G.M., Huey, R., Lindstrom, W., Sanner, M.F., Belew, R.K., Goodsell, D.S. and Olson, A.J. (2009) AutoDock4.2 andAutoDock Tools4: Automated docking with selective receptor flexibility. *J. Comput. Chem.* 30, 2785-2791.
17. Prashanth G.K and G.M. Krishnaiah (2014). Chemical composition of the leaves of *Azadirachta indica Linn* (Neem). *International Journal of Advancement in Engineering Technology Management and Applied Science.* Vol 1(5): 21-31